

20. I. Kuscer, "Reciprocity in scattering of gas molecules by surfaces," *Surface Sci.*, 25, No. 2 (1971).
21. M. N. Kogan and N. K. Makashev, "Construction of gas dynamics equations for multiatomic gases with an arbitrary ratio of the rates and elastic and inelastic processes," *Izv. Akad. Nauk SSSR, Mekh. Zhidk. Gaza*, No. 2 (1978).
22. V. V. Struminskii, "Effect of the diffusion rate on flow of gaseous mixtures," *Prikl. Matem. Mekh.*, 38, No. 2 (1974).

CONSIDERATION OF VARIABLE VISCOSITY IN THE DYNAMICS OF SOILS
AND POROUS MULTICOMPONENT MEDIA

G. M. Lyakhov

UDC 624.131+539.215

Analysis of tests indicates that the bulk viscosity of soils, rocks, ice, and snow is not a constant of the medium, but varies in the loading process.

The model of a solid nonlinear viscoplastic multicomponent medium, intended to describe wave processes [1], is refined below by the introduction of variable bulk viscosity. It is assumed that the viscosity varies (increases) as the state of the medium shifts from a dynamic to a static bulk-compression diagram under load. With this approach, wave processes are described by a system of hyperbolic quasi-linear equations in partial derivatives, just as for constant viscosity. This makes it possible to solve a broad class of wave problems.

1. Determination of Bulk Viscosity from Experimental Data. The variation in the bulk-viscosity coefficient η_L as a function of the loading regime has been noted in many experimental studies. Lyakhov [2] indicates that the η_L of a sandy soil increases by a factor of five as the rise time of the blast loading increases by a factor of three. In rocks [3], the viscosity increases by a factor of 10 as the duration of the load increases under the same stress level. At the same time, the viscosity decreases with increasing stress. For similar maximum stresses in loess and clayey soils, η_L increases by several factors as the loading rate decreases [1, 4].

Let us examine the results of tests [5, 6] in which the spread velocity c and absorption decrement Δ of plane waves of different frequency f , created by a sinusoidal load in frozen soils and in ice, and from which it is possible to determine the viscosity, and the law governing its variation as a function of loading regime, were determined.

The tests corresponded to small strains ϵ ranging from 10^{-7} to $5 \cdot 10^{-4}$. In this region, the nonlinearity of the limiting compression diagrams and strain irreversibility can be neglected, and the model of a standard linear body can be used, if the viscosity is considered constant. In the case of a uniaxial strain state, the equation of compression and unloading assumes the form

$$\dot{\epsilon} - \frac{\dot{\sigma}}{E_D} - \frac{\mu(\sigma - E_S \epsilon)}{E_S} = 0, \quad (1.1)$$

where $E_D = c_D^2 \rho_0$, and E_S are the limiting dynamic (when $\dot{\sigma} \rightarrow \infty$) and static (when $\dot{\sigma} \rightarrow 0$) compression moduli, respectively, μ is a viscosity parameter, c_D is the wave velocity when $f \rightarrow \infty$, ρ_0 is the initial density of the medium, and σ is the stress component in the direction of wave propagation. The factor η_L is linked to the viscosity parameter in the following manner:

$$\eta_L = E_S(E_D - E_S)/E_D \mu = E_D(\gamma - 1)/\gamma^2 \mu, \quad \gamma = E_D/E_S. \quad (1.2)$$

During wave propagation, nonsteady oscillations, which convert gradually to steady-state oscillations, develop in the medium. The extinction rate of the amplitude σ of the steady-

state oscillations is determined by the absorption decrement

$$\Delta = \alpha c / 2\pi f, \alpha = \ln(\sigma_{i-1}/\sigma_i) / (r_i - r_{i-1}) \quad (1.3)$$

(i is the number of the point of the medium, c is the velocity of the steady-state oscillations, and r is distance).

In a standard linear body, Δ and $\mu/2f$ are related by the equation [7]

$$\frac{\mu}{2f} = \frac{\pi}{4\gamma\Delta} [\gamma - 1 - \sqrt{(\gamma - 1)^2 - 16\gamma\Delta^2}]. \quad (1.4)$$

Having determined Δ from experiment, it is then possible to find μ for known γ and f [7].

Experimental values of c and Δ for different frequencies, which correspond to the region of steady-state oscillations [5, 6] ($E = c^2\rho_0$ is the current compression modulus) are presented in Table 1. The characteristics of the media investigated are as follows: 1) ice, $\rho_0 = 900-904 \text{ kg/m}^3$, temperature $T = -4^\circ\text{C}$, $E_D = 8.7 \cdot 10^9 \text{ N/m}^2$, and $\gamma = 2$; 2) ice, $\rho_0 = 770 \text{ kg/m}^3$, $T = -4^\circ\text{C}$, $E_D = 6.1 \cdot 10^9 \text{ N/m}^2$, and $\gamma = 2.5$; 3) silty Alaska and Manchester soils, $\rho_0 = 1980 \text{ kg/m}^3$, moisture content $w \sim 0.14$, $T = -4^\circ\text{C}$, $E_D = 18.5 \cdot 10^9 \text{ N/m}^2$, and $\gamma = 7.5$; 4) Ottawa sand, $\rho_0 = 2035 \text{ kg/m}^3$, $w = 0.12$, $T = -4^\circ\text{C}$, $E_D = 39 \cdot 10^9 \text{ N/m}^2$, and $\gamma = 4.4$; 5) silty soil, $\rho_0 = 1950 \text{ kg/m}^3$, $w = 0.2$, $T = -1^\circ\text{C}$, $E_D = 8.4 \cdot 10^9 \text{ N/m}^2$, and $\gamma = 6$; 6) same soil, $T = -10^\circ\text{C}$, $E_D = 24 \cdot 10^9 \text{ N/m}^2$, and $\gamma = 2.5$.

In conformity with (1.4), μ and η_L , which are listed in Table 1, are determined from the Δ and f values. It follows from these data that the viscosity parameter and the coefficient of viscosity of frozen soils and ice are not constants of their respective medium. Each f value has a corresponding value of μ and η_L . μ decreases, and η_L increases with decreasing frequency. The variation in both values attains several orders of magnitude. The model of the standard-linear body must be refined by the introduction of variable viscosity. The wave velocity and $E = c^2\rho_0$ vary with vibration frequency; this makes it possible to represent μ and η_L as functions of E/E_D . $\eta_L = \eta_L(E/E_D)$ curves 1-10 are shown in Fig. 1 (their numbers correspond to the media in Tables 1 and 2).

TABLE 1

Medium	f , Hz	c , m/sec	$E \cdot 10^{-9}$, N/m ²	Δ	μ , sec ⁻¹	η_L , (N·sec)/m ²
1	0,1	2200	4,35	0,07	0,09	$2,2 \cdot 10^{10}$
	10	2300	4,7	0,03	3,8	10^9
	1000	2570	7,9	0,03	380	$5,6 \cdot 10^8$
	5000	3000	8,1	0,02	1570	$1,3 \cdot 10^8$
	10000	3080	8,6	0,02	1970	$1,1 \cdot 10^8$
2	0,3	2050	3,1	0,045	0,18	$1,5 \cdot 10^{10}$
	1	2100	3,3	0,03	0,44	$1,2 \cdot 10^{10}$
	6	2110	3,4	0,03	2,7	$2,6 \cdot 10^9$
3	0,1	1100	2,5	0,23	0,04	$5 \cdot 10^{10}$
	1	1200	3,0	0,22	0,26	$5,2 \cdot 10^9$
	10	1800	6,7	0,13	2,5	$9 \cdot 10^8$
	1000	2900	16,5	0,03	44	$4,8 \cdot 10^7$
	5000	2950	17,2	0,022	95	$2,2 \cdot 10^7$
	10000	3000	17,8	0,02	380	$5,5 \cdot 10^6$
4	0,1	2150	9,4	0,17	0,02	$1,1 \cdot 10^{11}$
	6	2300	11	0,06	1,3	$5,4 \cdot 10^9$
	1000	3900	31	0,045	140	$4,8 \cdot 10^7$
	5000	4150	35	0,03	530	$1,3 \cdot 10^7$
	10000	4200	37	0,02	980	$7,4 \cdot 10^6$
5	0,05	860	1,4	0,26	0,03	$2,3 \cdot 10^{10}$
	1,0	1060	2,2	0,19	0,5	$2,3 \cdot 10^9$
	10	1240	3,0	0,13	3,4	$2,4 \cdot 10^8$
6	0,05	2240	9,8	0,09	0,04	$1,4 \cdot 10^{11}$
	1,0	2430	11,5	0,07	0,6	$9,6 \cdot 10^9$
	10	2730	14,5	0,04	3,4	$1,7 \cdot 10^9$

TABLE 2

Medium	$\dot{\sigma} \cdot 10^{-5}$, N/(m ² ·sec)	ε	E/E_D	μ , sec ⁻¹	$\eta_L \cdot 10^{-4}$, (N·sec)/m ²
7	2 000	0,034	0,34	630	2,3
	8 160	0,027	0,43	1700	0,9
	13 900	0,02	0,58	2200	0,7
	30 200	0,019	0,61	4500	0,3
8	7 040	0,052	0,26	1300	0,7
	13 800	0,034	0,39	1600	0,5
	40 300	0,020	0,67	3000	0,2
9	4 300	0,042	0,26	500	2,2
	18 300	0,03	0,37	2100	0,5
	43 900	0,021	0,53	3400	0,2
10	2 500	0,01	0,33	400	9,2
	15 000	0,006	0,55	1300	2,8
	20 000	0,004	0,83	2200	1,6

Using the experimental data, let us find η_L at a positive temperature. Vovk et al. [4], and Rykov and Skobeev [8] compressed specimens in an impulse machine in a uniaxial strain state for loadings rate $\dot{\sigma}$ that were different, but approximately constant in each test. The strains were measured under different stresses. The characteristics of the media investigated are presented in Table 2: 7) Kerchensk clay, $\rho_0 = 1850 \text{ kg/m}^3$, $w = 0.23$, $E_D = 8.6 \cdot 10^7 \text{ N/m}^2$, and $\gamma = 4.5$; 8) Kerchensk clay, $\rho_0 = 1840 \text{ kg/m}^3$, $w = 0.15$, $E_D = 7.5 \cdot 10^7 \text{ N/m}^2$, and $\gamma = 7.5$; 9) clayey soil, $\rho_0 = 1830 \text{ kg/m}^3$, $w = 0.13$, $E_D = 9 \cdot 10^7 \text{ N/m}^2$, and $\gamma = 7$; 10) loess-like clayey soil, $\rho_0 = 1450 \text{ kg/m}^3$, $w = 0.035$, $E_D = 3 \cdot 10^8 \text{ N/m}^2$, and $\gamma = 7$; the data from media 7-9 correspond to [4], and the data from media 10 to [8] (the γ values are approximate). The results of the tests - the $\dot{\sigma}$ and ε values - correspond to $\sigma = 10 \cdot 10^5 \text{ N/m}^2$.

The limiting compression diagrams of the medium can be assumed linear. From (1.1) when $\dot{\sigma} = \text{const}$, we then have an equation, which when integrated for the initial condition ($t = 0$) $\varepsilon = 0$, the stress-strain relationship

$$\frac{\varepsilon - \sigma/E_S}{1 - e^{-\mu\sigma/\dot{\sigma}}} = - \frac{\dot{\sigma}}{E_S \mu} \frac{\gamma + 1}{\gamma}$$

can be determined. The value of μ is determined from this equation. The resultant μ and η_L values are presented in Table 2. It is assumed that $\sigma/\varepsilon E_D = E/E_D$.

Curves 7-10 in Fig. 1 correspond to the $\eta_L = \eta_L(E/E_D)$ curve in unfrozen soils. Analysis of the experimental data indicate that the η_L of the unfrozen soils is not a constant of the medium. η_L increases with decreasing ratio $\sigma/\varepsilon E_D = E/E_D$; this corresponds to a shift of the state of the medium from the dynamic to the static compression diagram in the σ, ε plane. η_L is the ultimate value on the dynamic diagram.

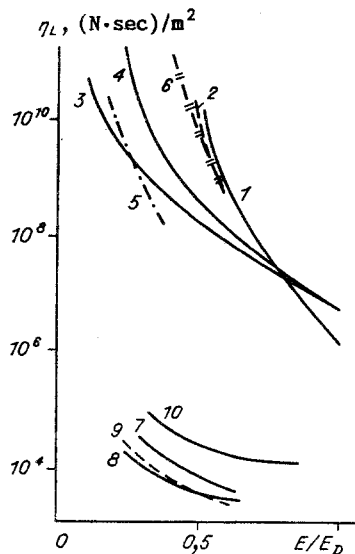


Fig. 1

The values of η_L depend heavily on the properties of the medium - the gradation, porosity, moisture content, and temperature. In slightly moist loess-like clayey soil (medium 10), cementation of the mineral particles, which characterizes the strength properties of the soil, is greater than that in the more moist soils (media 7-10). This dictates the high values of E_D and η_L .

Gradual freezing of pore water occurs with decreasing temperature; in this case, the strong bonds between the mineral particles increase, E_D increases by several times, and η_L by several orders of magnitude. E_D increases by a factor of approximately three, and η_L by two and one half orders of magnitude when the temperature of the silty soil drops from -1 to -10°C (media 5 and 6). η_L is several orders of magnitude higher in the frozen soils and ice than in the unfrozen soils.

The reduction in γ occurs simultaneously with increasing E_D , i.e., the difference between the limiting dynamic and static compression moduli is reduced; this leads to a reduction in energy losses during wave propagation. The curve of η_L versus E/E_D in the loading process can be represented as

$$\eta_L = \eta_{LD} (E/E_D)^{-m}, m > 1. \quad (1.5)$$

Each value of E has its own value of η_L .

In this connection, it is proposed that model (1.1) of a standard linear body be refined by introducing variable viscosity, and that the compression and unloading equation assume the form

$$\dot{\epsilon} - \frac{\dot{\sigma}}{E_D} - \mu_D \left(\frac{\sigma}{\epsilon E_D} \right)^m \frac{\sigma - E_S \epsilon}{E_S} = 0, \mu_D = \frac{E_D (\gamma - 1)}{\gamma^2 \eta_{LD}}, \frac{\sigma}{\epsilon E_D} = \frac{E}{E_D}. \quad (1.6)$$

Like (1.1), Eq. (1.6) applies to the region of small loads, when the limiting diagrams can be assumed linear.

Values of η_{LD} and m of the media investigated are presented in Table 3. The variation in η_L during loading was considered previously in models of the media. Lyakhov [9] proposes a model for a liquid and saturated soil containing gas bubbles. It is assumed that during wave processes, the coefficient of viscosity increases on compression of the bubbles, i.e., with increasing deformation of the medium.

In describing the behavior of the soils and ice [10-12], η_L is considered to increase with increasing loading time. Gold and Sinkha [11] recommend the following equations, which in our notations, assume the following form, in lieu of (1.1) to describe the behavior of ice:

$$\dot{\epsilon} - \frac{\dot{\sigma}}{E_D} - \frac{\mu}{t^{2/3}} \frac{\sigma - E_S \epsilon}{E_S} = 0.$$

The tests indicate, however, that $\eta_L \neq 0$ at the initial time. The description of the deformation mechanism will apparently be more accurate, if η_L is treated as a functional defined by the entire load history. In this case, difficulties arise with the derivation of material functions for the model and with computer-assisted solution of wave problems.

The proposed accounting of variable viscosity (Eq. (1.6)) as a function of the ratio E/E_D is approximate; it reflects, however, the basic laws of the variation in η_L .

TABLE 3

Media	$\eta_{LD} \cdot 10^{-5}$ (N·sec)/m ²	m	Media	$\eta_{LD} \cdot 10^{-5}$ (N·sec)/m ²	m
1	10	14	6	9	14
2	10	13	7	0,02	2,3
3	54	4,5	8	0,015	1,5
4	70	6,5	9	0,013	2,0
5	1.1	7.5	10	0.1	2,1

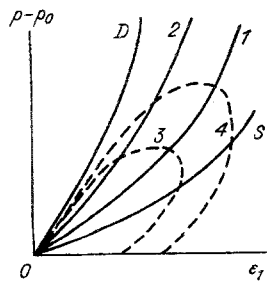


Fig. 2

2. Refinement of Model of Multicomponent Medium With Nonlinear Limiting Diagrams.

In Lyakhov's model [1], it is assumed that the bulk deformation of multicomponent media - soils, ice, snow - is summed from the strain ϵ_1 of the free pore space and the strains ϵ_2 , ϵ_3 , and ϵ_4 of the material of the liquid component, solid mineral particles, and ice, respectively:

$$\epsilon = \sum_{i=1}^4 \alpha_i \epsilon_i, \quad \sum_{i=1}^4 \alpha_i = 1,$$

where α_1 , α_2 , α_3 , and α_4 are the volumes of the free pore space, water, mineral particles, and ice in a unit volume of the medium. $\alpha_4 = 0$ in unfrozen soils, and $\alpha_2 = 0$ and $\alpha_3 = 0$ in ice and snow.

The deformation ϵ_1 , which is associated with the displacement and restacking of solid and liquid particles, does not take place instantaneously. This leads to a difference in the limiting dynamic and static bulk-compression diagrams of the free pore space. The diagrams are approximated by the equations

$$p - p_0 = f_S(\epsilon_1) = \frac{\rho_0 c_S^2}{\gamma_S} [(\epsilon_1 + 1)^{-\gamma_S} - 1] \quad \text{when } \dot{p} \rightarrow 0,$$

$$p - p_0 = f_D(\epsilon_1) = \frac{\rho_0 c_S^2}{\gamma_S} [(\epsilon_1 + 1)^{-\gamma_S} - 1] + k\epsilon \quad \text{when } \dot{p} \rightarrow \infty, \quad k < 0.$$

The equations for the compression of the material of the remaining components is independent of loading rate:

$$p - p_0 = f(\epsilon_i) = \frac{\rho_i c_i^2}{\gamma_i} [(\epsilon_i + 1)^{-\gamma_i} - 1], \quad i = 2, 3, 4.$$

In conformity with these experimental data in the region of small stresses, where the limiting diagrams are linear, η_L can be assumed approximately constant along the lines $\sigma = E\epsilon$.

Let us assume that in the case of nonlinear limiting diagrams, the coefficient η_L is constant along the curves

$$p - p_0 = \frac{\rho_0 c_S^2}{\gamma_S} [(\epsilon_1 + 1)^{-\gamma_S} - 1] + \kappa \epsilon_1, \quad \kappa \leq 0, \quad |\kappa| \leq |k|, \quad (2.1)$$

which fall between limiting diagrams. The variation in η corresponds to an equation similar to (1.5):

$$\eta = \eta_D \left(\frac{-\rho_0 c_S^2 + \kappa}{-\rho_0 c_S^2 + k} \right)^{-m}. \quad (2.2)$$

In Fig. 2, D and S are the limiting dynamic and static compression diagrams of the free pore space, 1 and 2 are lines of constant η , which are described by (2.1), and 3 and 4 are diagrams that are realized with the passage of waves. The smallest η_D and largest η_S are attained on the dynamic and static diagrams, respectively:

$$\eta_S = \eta_D \frac{-\rho_0 c_S^2 + k}{-\rho_0 c_S^2}.$$

It follows from (2.1) and (2.2) that

$$\eta = \eta_D \left[\frac{-\rho_0 c_S^2 + \frac{p-p_0-f_S(\varepsilon_1)}{\varepsilon_1}}{-\rho_0 c_S^2 + k} \right]^{-m} = \eta_D \left[\frac{-\rho_0 c_S^2 + \frac{\psi(p, V)}{\varepsilon_1}}{-\rho_0 c_S^2 + k} \right]^{-m}. \quad (2.3)$$

The equation of the bulk compression of a medium [1] assumes the form

$$\dot{\varepsilon} = \frac{\dot{V}}{V_0} = \varphi(p, V) \dot{p} - \frac{\alpha_1 \lambda(p, V)}{\eta} \dot{\psi}(p, V), \quad (2.4)$$

where

$$\varphi(p, V) = \alpha_1 \left(\frac{df_D}{d\varepsilon_1} \right)^{-1} - \sum_{i=2}^4 \frac{\alpha_i}{\rho_i c_i^2} \left[\frac{\gamma_i (p-p_0)}{\rho_i c_i^2} + 1 \right]^{-(1+\gamma_i)/\gamma_i};$$

$$\lambda(p, V) = \left(\frac{df_D}{d\varepsilon_1} \right)^{-1} \frac{df_S}{d\varepsilon_1}; \quad \psi(p, V) = p - p_0 - f_S(\varepsilon_1);$$

$$f_S(\varepsilon_1) = \frac{\rho_0 c_S^2}{\gamma_S} [(\varepsilon_1 + 1)^{-\gamma_S} - 1]; \quad f_D(\varepsilon_1) = f_S(\varepsilon_1) + k\varepsilon_1;$$

$$\varepsilon = (V - V_0)/V_0; \quad p - p_0 = -(\sigma_r + \sigma_\theta + \sigma_z)/3$$

(η corresponds to (2.3)). η_L is usually determined in tests. The coefficient η applies to the bulk strain of the free pore space, and η_L to the longitudinal compression of the medium on the whole under a stress σ_r . In conformity with this, the relation between them can be written as

$$\eta_L = \frac{3\eta}{\alpha_1(1+k_\theta+k_z)}, \quad k_\theta = \sigma_\theta/\sigma_r, \quad k_z = \sigma_z/\sigma_r.$$

In Lyakhov's model [1], it is assumed that the equations of component unloading conform to the equations of loading (2.4). Unloading of the free pore space occurs in accordance with the equation

$$\varepsilon_1 + 1 = \left[\frac{\gamma_R(p-p_0)}{\rho_0 c_R^2} + 1 \right]^{-1/\gamma_R} + \left[\frac{\gamma_S(p_m-p_0)}{\rho_0 c_S^2} + 1 \right]^{-1/\gamma_S} - \left[\frac{\gamma_R(p_m-p_0)}{\rho_0 c_R^2} + 1 \right]^{-1/\gamma_R}, \quad \gamma_R \geq \gamma_S.$$

It begins when $|\varepsilon_1|$ attains the maximum value $|\varepsilon_{1m}|$ when $p = p_m$. On these premises, the equation of bulk unloading assumes the form of (2.4). The determining equations are:

$$\varphi(p, V) = \alpha_1 \left(\frac{df_D}{d\varepsilon_1} - \frac{df_S}{d\varepsilon_1} + \frac{df_R}{d\varepsilon_1} \right)^{-1} - \sum_{i=2}^4 \frac{\alpha_i}{\rho_i c_i^2} \left[\frac{\gamma_i (p-p_0)}{\rho_i c_i^2} + 1 \right]^{-(1+\gamma_i)/\gamma_i},$$

$$\lambda(p, V) = \left(\frac{df_D}{d\varepsilon_1} - \frac{df_S}{d\varepsilon_1} \right) \left(\frac{df_D}{d\varepsilon_1} - \frac{df_S}{d\varepsilon_1} + \frac{df_R}{d\varepsilon_1} \right)^{-1},$$

$$f_R(\varepsilon_1) = \frac{\rho_0 c_R^2}{\gamma_R} \left\{ \left[\varepsilon_1 + 1 - \left(\frac{\gamma_S(p_m-p_0)}{\rho_0 c_S^2} + 1 \right)^{-1/\gamma_S} + \left(\frac{\gamma_R(p_m-p_0)}{\rho_0 c_R^2} + 1 \right)^{-1/\gamma_R} \right]^{-\gamma_R} - 1 \right\}.$$

During unloading, η is considered constant, and its value corresponds to that achieved when $\varepsilon_1 = \varepsilon_{1m}$. If the point $p_m - p_0$, ε_{1m} lies beyond the static-compression diagram, $\eta = \eta_S$.

The Mises-Schleiker plasticity condition is used in the form

$$S_r = \frac{k^*(p-p_0)}{1+k^*(p-p_0)/(p^*-p_0)}, \quad S_r = \sigma_r + p - p_0. \quad (2.5)$$

when $p - p_0 \rightarrow 0$, $p - p_0 = p^* - p_0$, and $p - p_0 \rightarrow \infty$, the lateral-pressure coefficient k_θ is $(2 - k^*)/2(k^* + 1)$, $(2 + k^*)/2(2k^* + 1)$, and 1, respectively [13, 14].

In solving problems with cylindrical symmetry, it is assumed that

$$\sigma_z = (\sigma_r + \sigma_\theta)/2. \quad (2.6)$$

The constants of the medium are determined experimentally.

Together with the basic equations of motion of a continuum, equations (2.4)-(2.6) form a closed system, which makes it possible to solve wave problems with plane, spherical, and cylindrical waves on a computer with allowance for variable viscosity by the same methods that are used for constant viscosity.

Problems of wave propagation in a nonlinear multicomponent medium are solved in [13-15] for a constant viscosity in accordance with Lyakhov's model [1]. Calculations indicate that the maximum stress of a spherical blast wave when $\sigma_r \sim 10 \cdot 10^5$ N/m² changes by 30-40% when the constant value of η is increased by a factor of 50. If a certain median value, which falls between η_g and η_d is adopted as the constant value of η , deviations from the calculations for a variable viscosity will apparently be of the same order. It should be noted that the effect of the variation in η on the parameters of a wave depends on its length, and on the mass of the charge in the case of a blast wave. This should manifest itself in deviations of wave parameters from laws of similitude.

LITERATURE CITED

1. G. M. Lyakhov, Waves in Soils and Porous Multicomponent Media [in Russian], Nauka, Moscow (1982).
2. G. M. Lyakhov, "Determination of the viscous properties of soils," Zh. Prikl. Mekh. Tekh. Fiz., No. 4 (1968).
3. I. V. Belinskii, A. V. Mikhalyuk, and B. D. Khristoforov, "Viscosity of rocks during deformation processes," Izv. Akad. Nauk SSSR. Fiz. Zemli, No. 8 (1975).
4. A. A. Vovk, A. V. Mikhalyuk, and G. I. Chernyi, Effect of Large-Scale Blasts in a Rock Mass [in Russian], Naukova Dumka, Kiev (1974).
5. T. S. Vinson, "Parameter effects on dynamic properties of frozen soils," Proc. Am. Soc. Civ. Eng. J. Geotechn. Engng. Div., 104, No. 10 (1978).
6. R. L. Chaykowski and T. S. Vinson, Dynamic properties of frozen silt under cyclic loading," Proc. Am. Soc. Civ. Eng. J. Geotechn. Engng. Div., 106, No. 9 (1980).
7. S. Ya. Kogan, Seismic Energy and Methods of its Determination [in Russian], Nauka, Moscow (1975).
8. G. V. Rykov and A. M. Skobeev, Stress Variation in Soils Under Short-Term Loadings [in Russian], Nauka, Moscow (1978).
9. A. G. Lyakhov, "Wave interaction in a multicomponent dual-phase medium with a barrier," Izv. Akad. Nauk SSSR, Mekh. Zhidk. Gaza, No. 3 (1981).
10. A. V. Mikhalyuk, Rocks Under Nonuniform Dynamic Loads [in Russian], Naukova Dumka, Kiev (1980).
11. L. Gold and N. Sinkha, "Rheologic behavior of ice during small deformations," in: Physics and Mechanics of Ice [Russian translation], Mir, Moscow (1983).
12. V. V. Nefedov, "Plane waves in nonlinear viscous multicomponent media," Zh. Prikl. Mekh. Tekh. Fiz., No. 6 (1987).
13. A. V. Krymskii and G. M. Lyakhov, "Waves induced by underground blasting," Zh. Prikl. Mekh. Tekh. Fiz., No. 4 (1984).
14. S. S. Grigoryan, A. V. Krymskii, and G. M. Lyakhov, "Problems of wave similitude in porous multicomponent media," Izv. Akad. Nauk SSSR, Mekh. Tverd. Tela, No. 6, (1985).
15. G. M. Lyakhov, I. A. Luchko, V. A. Plaksii, et al., "Spherical blast waves in a solid multicomponent viscoplastic medium," Prikl. Mekh., No. 5 (1986).